Design and Fabrication of Piezoelectric Micromachined Ultrasound Transducer (pMUT) with Partially-Etched ZnO Film

Junhong Li *, Wei Ren, Guoxiang Fan and Chenghao Wang

State Key Laboratory of Acoustics, Institute of Acoustics, Chinese Academy of Science, Beijing 100190, China; renwei@mail.ioa.ac.cn (W.R.); fanguoxiang13@mails.ucas.ac.cn (G.F.); chwang@mail.ioa.ac.cn (C.W.)

* Correspondence: ljh@mail.ioa.ac.cn; Tel.: +86-10-8254-7816

Abstract: A square piezoelectric composite diaphragm was analyzed by the finite element method to enhance the sensitivity of a piezoelectric micromachined ultrasound transducer (pMUT). The structures of electrode and piezoelectric film were optimized and a centric electrode was designed to avoid the counteraction of stress in the centre and edges. In order to further improve the sensitivity; a pMUT with partially-etched piezoelectric film was adopted. The receive and transmit sensitivities of the pMUT were analyzed in details. The receive sensitivity of pMUT with partially-etched ZnO film is 3.3 dB or 6.8 dB higher than those with a centric and whole electrode, respectively; and the amplitude of a partially-etched ZnO film pMUT under a certain voltage is 5.5 dB and 30 dB higher than those with centric and whole electrode separately. Two pMUT-based ZnO films were fabricated by micromachining technology and their receive and transmit sensitivities were tested. The ZnO films deposited by direct current (DC) magnetron sputtering exhibit a densely packed structure with columnar crystallites. The test results show that the structure of the square diaphragm with partially-etched piezoelectric layer can significantly improve the transducer sensitivity. The receive sensitivity and transmit sensitivity are −238.35 dB (ref. 1 V/μPa) and 150.42 dB (ref. 1 μPa/V); respectively.

Keywords: pMUT; centric electrode structure; ZnO film; partially-etched; sensitivity

1. Introduction

Micromachined ultrasound transducers (MUTs) have been extensively developed. Arrays with high element density, small element size and high resonant frequency are easy to realize by MUT [1–3]. Moreover, the MUT array and external circuit can be integrated in a chip. Therefore, MUT arrays have wide applications in medical acoustic imaging, ultrasonic fingerprint identification and ultrasonic vein identification [4–10]. The MUTs work on either electrostatic or piezoelectric principles, and they can be thus be classified as capacitive MUTs (cMUTs) and piezoelectric MUTs (pMUTs). Compared with cMUTs, pMUTs have lower impedance, which may allow more energy input and can avoid the DC-biased voltage cMUTs need [11,12]. The pMUT usually works in bending mode, and a few in extensional mode and d_{33} mode [13,14]. The properties of a MUT array depend greatly on the sensitivity of the single element transducers. The piezoelectric film and structure of pMUT are two important factors that affect the sensitivity. ZnO and PZT films are usually used as piezoelectric layers in pMUTs [15–20]. Compared with that of PZT film the deposition process of ZnO film is simple and compatible with micromachining technology [21–27]. In order to improve the properties of pMUT, Belgacem studied the influence of centred and ring top electrode on the coupling factor of pMUT with a circular piezoelectric composite diaphragm released by the expensive deep reactive

ion etch (DRIE) process, and they found that when the PZT was removed outside the electrode this can improve the coupling factor [28]. The vibration diaphragms of pMUTs include piezoelectric films and non-piezoelectric layers, and if released by wet etching they are square for anisotropic etching of silicon [29–31]. The wet etching process is simpler and cheaper than DRIE that can realize circular piezoelectric composite diaphragm. The theory analysis of square piezoelectric composite diaphragms is difficult to be carried out by analytical methods. The working process of pMUTs involves the transmission and reception of sound waves, thus the receive and transmit sensitivity of pMUTs need to be analyzed. In our work, a ZnO film was deposited by direct current (DC) magnetron sputtering and used as a piezoelectric material in a pMUT. As shown in Figure 1, the sensitivities of three kinds of pMUTs, including whole electrode, centric electrode and partially-etched ZnO film were analyzed by the finite element method (FEM), and a centric electrode and a partially-etched ZnO film were adopted to improve the sensitivity. Two pMUTs were designed and fabricated by a micromachining process. Finally, the sensitivities of pMUTs with partially-etched and whole ZnO films were tested and compared.
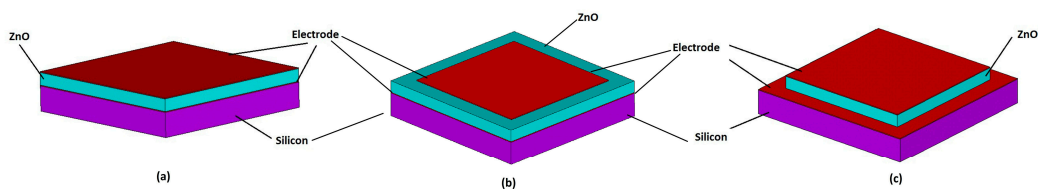

Figure 1. Schematic structure of pMUT's vibrating diaphragm with (**a**) whole electrode; (**b**) centric electrode and (**c**) partially-etching ZnO film.

2. Finite Element Analysis for a Piezoelectric Composite Diaphragm

The pMUT needs to work at a higher resonant frequency for an ultrasound imaging system with higher resolution, and the resonant frequency depends heavily on the thickness of the vibrating diaphragm. Silicon-on-insulator (SOI) wafers have accurate silicon layer thicknesses which usually ranges from several to dozens of microns, so they are suitable for pMUTs [32–34]. The control of bulk silicon etching time is another method to get a certain silicon layer thickness [2,14,30]. As shown in Figure 2, the piezoelectric composite vibrating diaphragm of a pMUT includes a non-piezoelectric vibration membrane and a piezoelectric film with top and bottom electrodes.
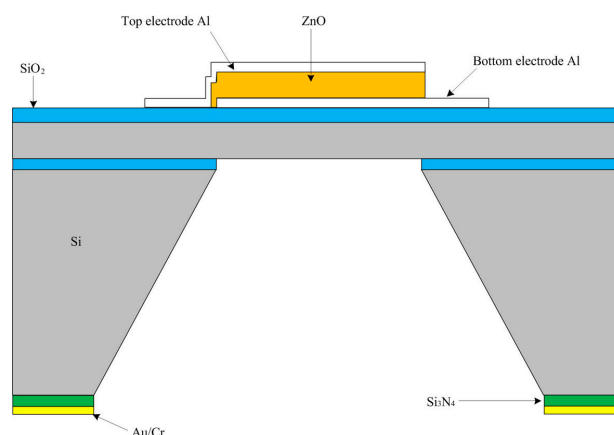

Figure 2. Schematic structure of the piezoelectric micromachined ultrasound transducer.

The resonant frequency of a pMUT is proportional to the thickness of the vibration diaphragm and piezoelectric film. Therefore, the thickness of the vibrating membrane is usually greater than 5 μm. The resonant frequency and sensitivities of three kinds of pMUTs, including whole electrode,

centric electrode and partially-etched ZnO films, were analyzed by the finite element method (FEM). The schematic structures of the pMUT's vibrating diaphragm with whole electrode, centric electrode and partially-etching ZnO film are shown in Figure 1. In finite element analysis, the up and bottom electrodes are 0.2 µm thick Al, and a 3 µm thick ZnO film is used as the piezoelectric layer. The piezoelectric composite vibrating diaphragm is square and 426 µm wide. The non-piezoelectric vibration diaphragm comprises 0.2 µm thick oxide and a 6 µm thick silicon device layer. The substrate silicon is 300 µm thick and anisotropically wet etched to release the vibrating diaphragm. In our work, the modal and static analysis of pMUT were studied by means of FEM using ANSYS. The eight-node hexahedral coupled-field element SOLID5 and the eight-node linear structural element SOLID45 were used for ZnO films and silicon, respectively. The structure parameters and properties of materials used in the FEM are listed in Table 1.

Table 1. Materials properties and thickness used in FEM simulation.

Materials	Young's Modulus (GPa)	Density (kg·m^{-3})	Poisson's Ratio	Thickness (µm)
ZnO	120	5.68	0.446	3
Si	167	2.33	0.28	6

In our FEM simulation, the effect of structural damping was neglected and the displacement degrees of freedom were constrained to be zero as the fixed four lateral faces of the piezoelectric ZnO/SiO$_2$/Si composite diaphragm that can be regarded as square thin plate. The vibration equation of a square composite thin plate can be written as:

$$\frac{\partial^4 w}{\partial x^4} + 2\frac{\partial^2 w}{\partial x^2 \partial y^2} + \frac{\partial^4 w}{\partial y^4} + \frac{\partial^2 w}{\partial t^2}\frac{\rho h}{D} = 0 \tag{1}$$

where w is the displacement, D is the bending rigidity, ρ and h are the average density and thickness of the composite diaphragm, respectively.

The modal analysis of the piezoelectric composite diaphragm was carried out to predict the resonant frequency, as shown in Figure 3. The resonant frequency of pMUT with whole and centric electrode are around 590 KHz, that is approximately equal to that calculated by the following expression [35]:

$$f_{11} = \frac{17.994}{\pi a^2}\sqrt{\frac{D}{\rho h}} \tag{2}$$

where D is the bending rigidity , ρ, a and h are is average density, length and thickness of the composite diaphragm respectively.
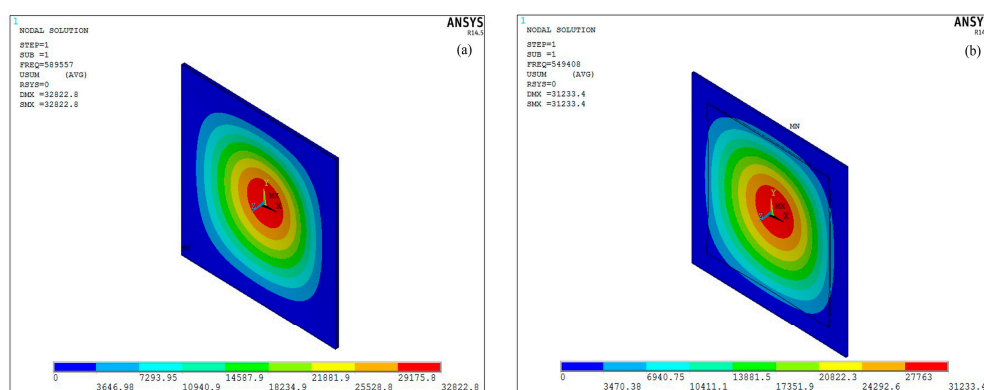

Figure 3. The displacement distributes of the piezoelectric composite diaphragm at first resonance mode (**a**) for whole or centric electrode and (**b**) for partially-etching ZnO film.

From the above expression, we can see that the resonant frequency of pMUT is proportional to thickness and inversely proportional to the width, respectively, which is in agreement with the results of other's research [2,14]. As shown in Figure 3b, the resonant frequency of a pMUT with partially-etching ZnO film is about 93% of that with a whole piezoelectric film.

The receive sensitivity *S* of pMUT can be calculated as [36]:

$$S = \frac{d_{31}}{\varepsilon A P} \int\limits_0^a \int\limits_0^a h\sigma dx dy \tag{3}$$

where *P* is the sound pressure on the pMUT, *A* and *a* are the area and length of the composite diaphragm separately, and *ε*, d_{31}, *h*, *σ* are the permittivity, piezoelectric (strain) coefficient , thickness and stress of the piezoelectric films, respectively. Due to the other parameters being equal, a greater stress means a higher receive sensitivity. To obtain the stress distribution in the piezoelectric composite diaphragms under uniform pressure load, a uniform pressure load (1 Pa) was imposed on composite diaphragm in FEM static analyses. As shown in Figure 4, the stress and displacement analyses were carried out along line P1 and P2. Figures 5 and 6 show the stresses distributions of pMUT with whole piezoelectric film. The stresses from edge to centric change gradually. The stresses in the centre and edge are bigger than in other areas, but they are opposite. Therefore, the partial stress will be offset if the electrodes cover the entire piezoelectric film, and the sensitivity of the pMUT will decrease.
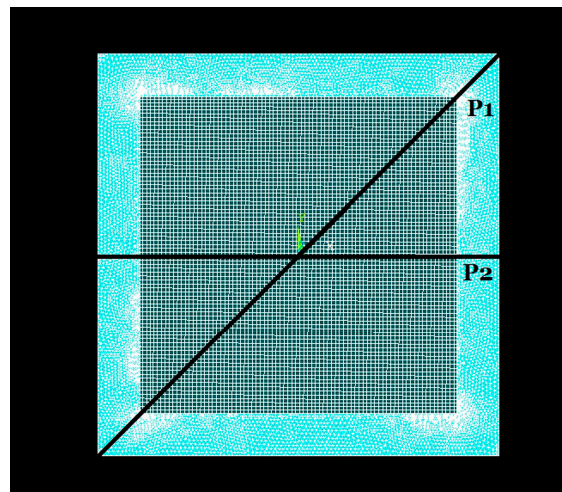

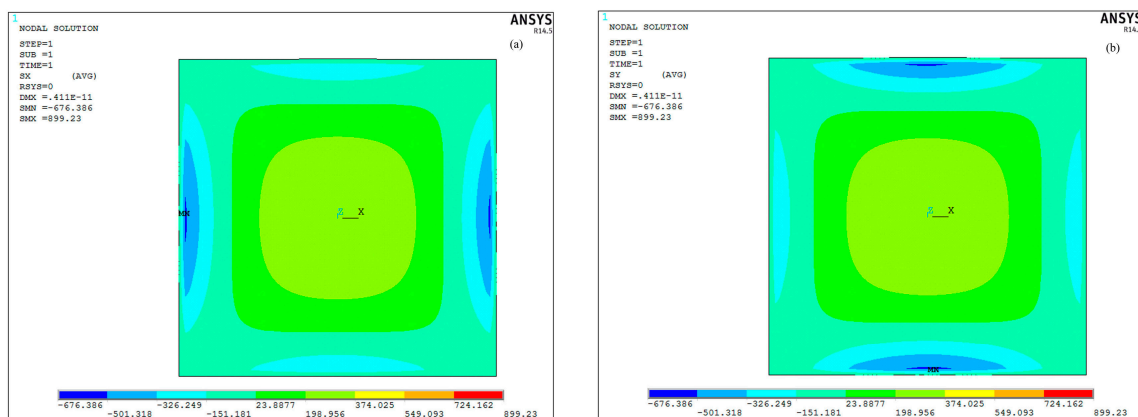**Figure 4.** The finite element mesh of the composite diaphragm.

Figure 5. The stress distributions of the piezoelectric composite diaphragm in (**a**) the X and (**b**) the Y direction.
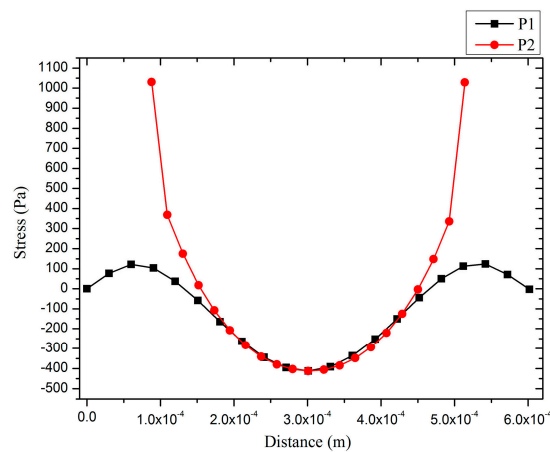
Figure 6. The stresses distributions in piezoelectric film of pMUT with whole electrode.

Figure 7 shows the stress distributions in the piezoelectric film with a centric electrode and partially-etched ZnO film. The average stress of the composite vibration diaphragm with centric electrode is higher by around 3.5 dB than those with a whole electrode by avoiding the counteraction of stress between the centre and out-ring regions. At the same time, the fact that ZnO film in the outer-ring region was etched leads to a further increase of the average stress in the piezoelectric film. The stress with partially-etching ZnO film is higher by around 3.3 dB and 6.8 dB than those with centric and whole electrodes, respectively, which means the receive sensitivity will increase by 3.3 dB and 6.8 dB.
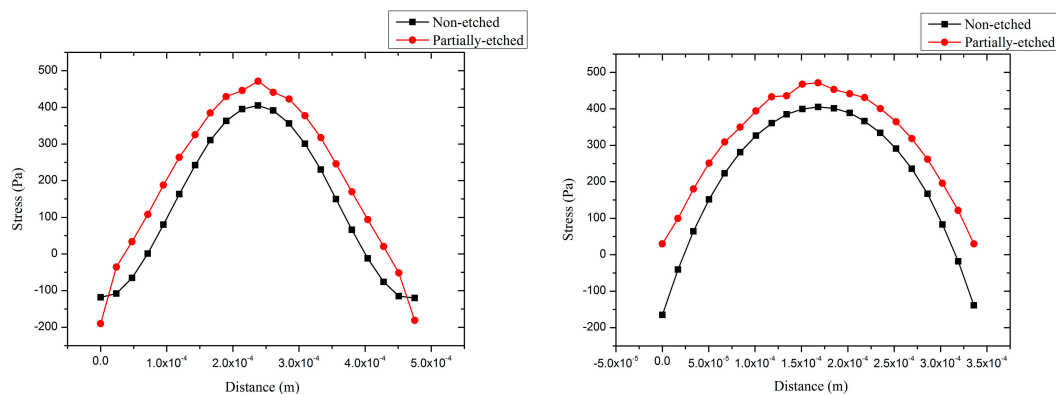

Figure 7. The stresses distributions in piezoelectric film of pMUT with whole and partially-etched ZnO films along P1 (**left**) and P2 (**right**) lines.

The transmit sensitivity of pMUT is proportional to the amplitude of the vibration diaphragm [30]. The amplitudes of pMUTs with whole, centric electrode and partially-etched ZnO films were compared by FEM static analysis, and a 1 V voltage was loaded on the piezoelectric film in the analyses. Figure 8 shows the amplitudes of pMUTs with whole electrode, centric electrode and partially-etching ZnO film. The amplitude of the pMUT with whole electrode is much lower than those with centric electrode and partially-etching ZnO film due to the offset of stress between the centric and out-ring regions. The amplitude of the pMUT with partially-etched ZnO film is higher by 5.5 dB than that with a whole piezoelectric film, which can be attributed to the change of boundary conditions of the vibrating diaphragm. In our work, two pMUTs with centric electrode and partially-etched ZnO film were fabricated, and their transmit and receive sensitivities were tested and compared.
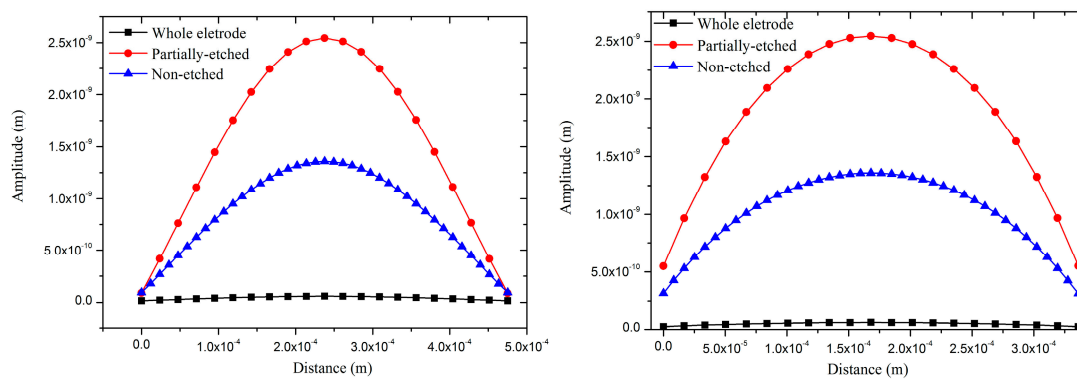
Figure 8. The amplitudes of pMUT with whole electrode, centric electrode and partially-etched ZnO films along P1 (**left**) and P2 (**right**) lines.

3. Microfabrication of pMUT

The pMUT has been fabricated using standard bulk micromachining fabrication techniques. Silicon nitride, silicon oxide and polysilicon are usually used as vibration diaphragms of MEMS devices, but the thicknesses of the three films are not more than 1 μm due to the deposition technique limits [37–40]. To get a higher and more accurate resonant frequency, the vibration diaphragm of pMUT should have greater and more precise thickness. Therefore, a layer of silicon got by controlling of bulk silicon etching time or SOI wafer was used as the vibration membrane of the pMUT (shown in Figure 9 is SOI wafer). The diaphragm was released by silicon anisotropic wet etching. The silicon anisotropic wet etching mask must be compact and anticorrosive to safeguard the wafer and successfully finish the pMUT microfabrication. On the basis of process experiments, a composite of Si_3N_4 deposited by plasma enhanced chemical vapor deposition (PECVD) and Au/Cr film was chosen as the mask.

A description of the pMUT microfabrication is shown in Figure 9. The wafers were firstly wet oxidized at 1100 °C to grow a 0.2 μm thick thermal oxide layer, which was removed from the back side of the wafer using hydrofluoric acid solution. A 0.5 μm thick silicon nitride film was then deposited by PECVD on the back side of the wafer to be used as the mask for the silicon anisotropic wet etching, followed by a 0.2 μm thick Al film deposited by ion-beam sputtering and patterned by standard photolithography techniques and wet etching in H_3PO_4 solution to form the bottom electrode. After that ZnO films were deposited on the bottom electrode, and patterned by a wet etching process using H_3PO_4 solution to finish the preparation of the piezoelectric layer. The effects of Ar/O_2 ratio and sputtering pressure on the properties of ZnO films deposited using dc magnetron sputtering were investigated, and the preparation parameters were optimized. As shown in Figure 10, the ZnO film exhibits a densely packed structure with columnar crystallites preferentially oriented along the (002) plane, which indicates the film possesses good piezoelectric properties. Following the preparation and patterning of the piezoelectric layer, a 0.2 μm thick Al film was deposited by ion-beam sputtering and photolithographically patterned by lift-off processing to form the top electrode. The Au/Cr film was then deposited on the back side of wafer and patterned by back-to-front alignment photolithography techniques and a wet etching process, followed by inductively coupled plasma dry etching of PECVD silicon nitride to form the mask for silicon wet etching. Thereafter, the wafer was fixed in a Teflon chucking appliance, and was anisotropically etched using a KOH etchant at 70 °C to release the diaphragm, The bulk silicon was wet etched until the required thickness was achieved, then the oxide was removed by hydrofluoric acid solution from the diaphragm. Finally, the wafer was unloaded from the fixture, and washed with deionized water.
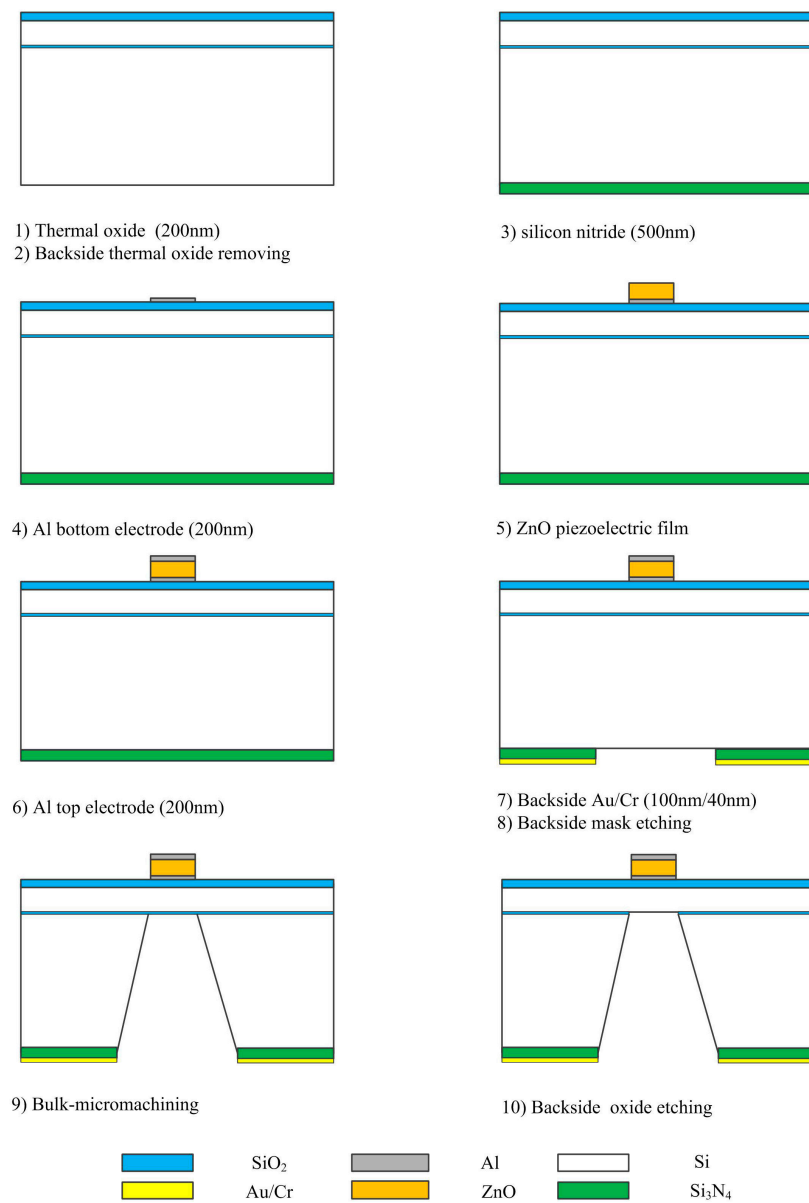
1) Thermal oxide (200nm)
2) Backside thermal oxide removing

3) silicon nitride (500nm)

4) Al bottom electrode (200nm)

5) ZnO piezoelectric film

6) Al top electrode (200nm)

7) Backside Au/Cr (100nm/40nm)
8) Backside mask etching

9) Bulk-micromachining

10) Backside oxide etching

| | SiO_2 | | Al | | Si |
| | Au/Cr | | ZnO | | Si_3N_4 |

Figure 9. Fabrication process of the pMUT.
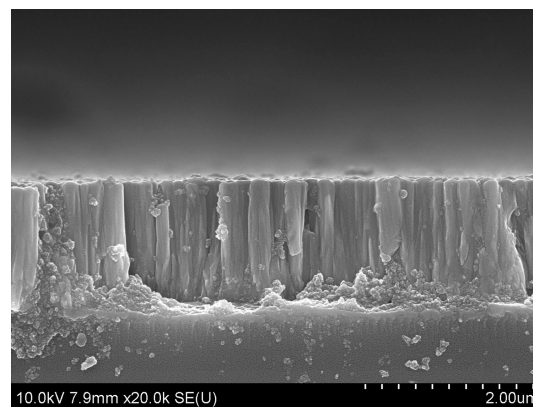

10.0kV 7.9mm x20.0k SE(U)   2.00um

Figure 10. SEM picture of the cross-section view of the ZnO films.

4. Results and Discussion

The pMUTs with whole and partially-etched ZnO film (the width of the square diaphragm is 470 μm, the thickness of ZnO, silicon oxide and silicon layers are 4, 0.2 and 33 μm, respectively) were fabricated by the above micromachining technique. As shown in Figure 11a, the ZnO films was partially etched, and the bottom electrode was also slightly etched during the process of removing of piezoelectric film. To measure the properties of devices, the pMUT dies were glued on a printed circuit board (PCB), electrically connected by ultrasonic pressure welding and packaged in metal box with a window where the vibration diaphragm of pMUT was exposed.
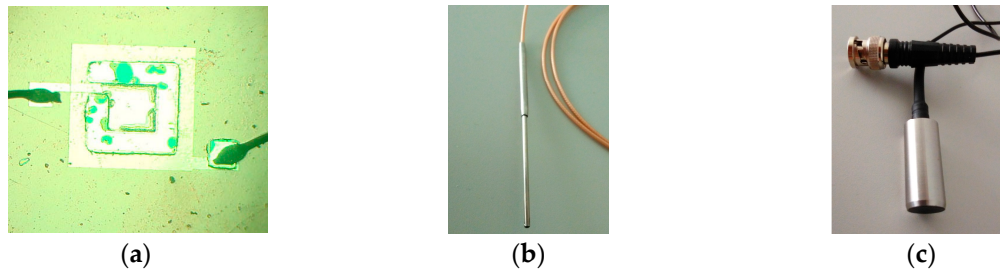

| (**a**) | (**b**) | (**c**) |

Figure 11. Optical images of (**a**) pMUT with partially-etched ZnO film and the calibrated (**b**) hydrophone; (**c**) transmit transducer used in sensitivity test.

The admittance curves of the pMUT were measured by a 4395A impedance phase analyzer (Agilent, Palo Alto, CA, USA). Figure 12 shows the admittance curves of pMUT with partially-etched piezoelectric film, where the resonant frequency in air is around 1.85 MHz. The measurements of both receive and transmit sensitivity were carried out in absolute ethanol. The receive sensitivity was measured by a comparison method as shown in Figure 13. The calibrated transducer (Figure 11c) in ten sine signals excitation transmits a sound wave at 1.79 MHz, and the pMUT and a calibrated hydrophone (Figure 11b) with 0.259 μV/Pa sensitivity were successively placed at the same position to receive the sound signal. The electric signals of hydrophone and pMUT were recorded by a TK DPO3012 oscilloscope (Tektronix, Beaverton, OR, USA).
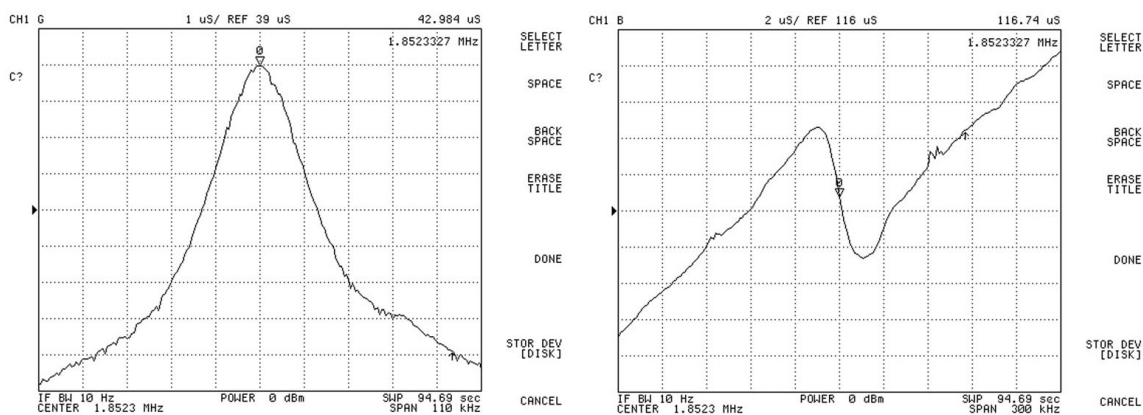

Figure 12. The admittance curves of pMUT with partially-etched ZnO film.

The pMUT with partially-etched ZnO film was used as transmit transducer in the measurement of transmit sensitivity as shown in Figure 13. The excitation generated by the TK AFG 3012 function generator is ten sine signals at 1.79 MHz, and the peak to peak value is 10 V. A calibrated hydrophone with a sensitivity of 0.259 μV/Pa was placed at a certain distance from the pMUT, and the received sound signal was recorded by the TK DPO 3012 oscilloscope. Figure 14 shows the measured results of receive sensitivity of the pMUT with partially-etched ZnO, where the voltage amplitude of the pMUT

and calibrated hydrophone are 9.9 mV and 2.12 mV, respectively, so the receive sensitivity of the pMUT is −238.35 dB (ref. 1 V/μPa), which is 3.05 dB higher than that with whole ZnO film.
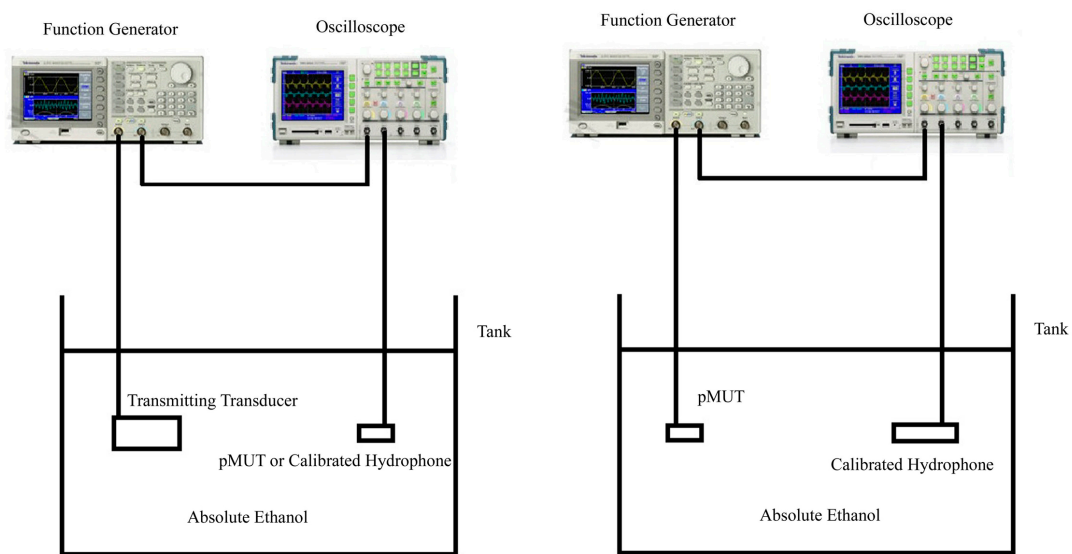

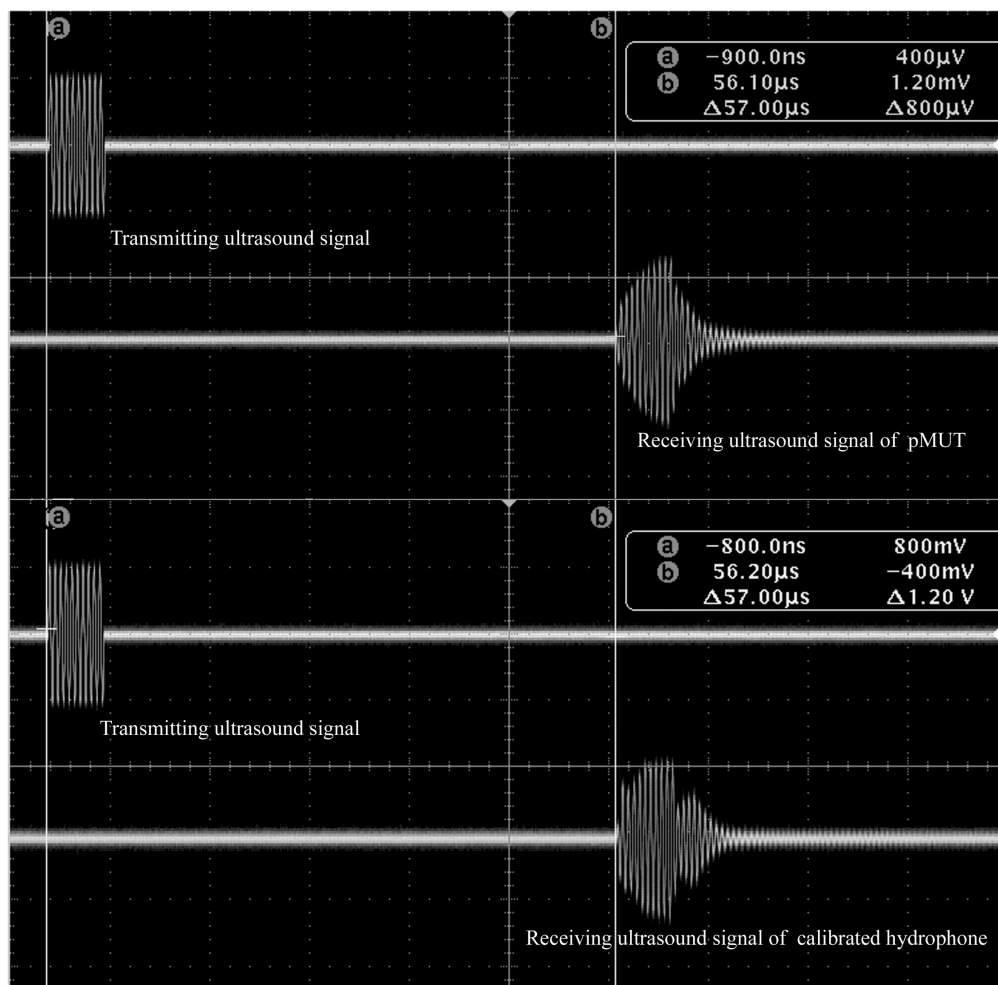**Figure 13.** Receive (**left**) and transmit (**right**) sensitivity test of a pMUT.

Figure 14. Measurement result of receiving sensitivity of a pMUT with partially-etched ZnO film.

Figure 15 shows the measured transmit sensitivity results of the pMUT with partially-etched ZnO. After calibration, the measured transmit sensitivity of the pMUT element is 33.189 Pa/V, i.e., 150.42 dB (ref. 1 µPa/V) at 20 mm equivalent distance, which is 8.78 dB higher than that of pMUT with whole ZnO films. Besides the simulation results, the increase of receive and transmit sensitivity can also be attributed to the piezoelectric property diversity of ZnO film on different wafers and the fact that etching of a partial piezoelectric film can decrease the residual stress ignored in the FEM analysis. The receive and transmit sensitivity of the pMUT with partially-etched ZnO films are comparable to those based on PZT films that have better piezoelectric performance than ZnO [41], which indicates the structure of partially-etched piezoelectric films can significantly improve the sensitivity.
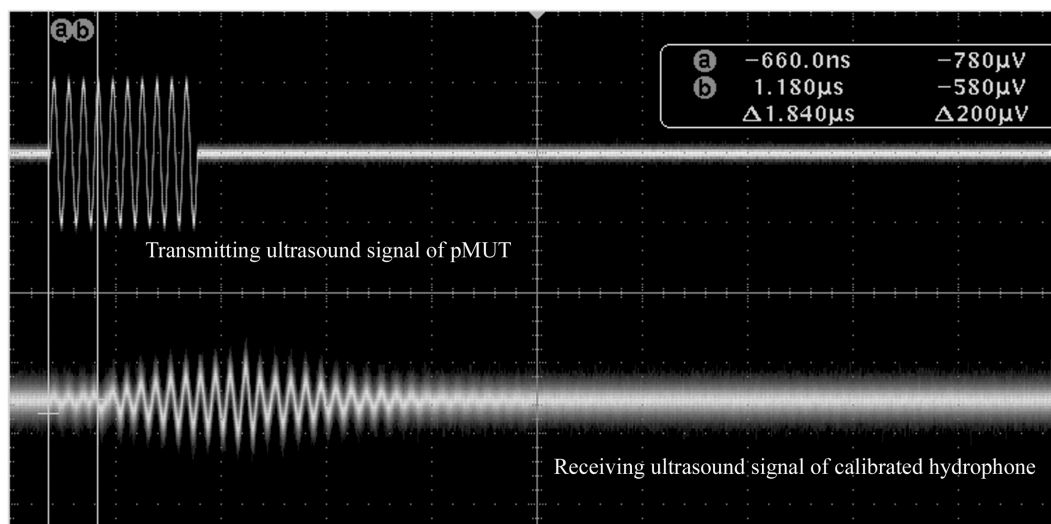

Figure 15. Measurement results of transmitting sensitivity of a pMUT with partially-etched ZnO film.

5. Conclusions

A square piezoelectric composite diaphragm of $ZnO/Si/SiO_2$ was analyzed by the finite element method. The resonant frequencies are approximately equal by the finite element method and plate vibration theory, and the simulation results show that the resonant frequency of the pMUT is proportional to its thickness and inversely proportional to its width, respectively. The stress distribution results show the stresses in the centre and edge of the square piezoelectric composite diaphragm are bigger than in other areas, but they are opposite. Therefore, a centric electrode was designed to avoid neutralization of the stress in the centre and edges. In order to further improve the sensitivity, a pMUT with partially-etched ZnO film was adopted in which unnecessary ZnO film in the outer-ring was removed. The resonant frequency and sensitivities of three kinds of pMUTs including whole electrode, centric electrode and partially-etched ZnO film were analyzed by the finite element method (FEM). The receive sensitivity of the pMUT with partially-etched ZnO film is 3.3 dB and 6.8 dB higher than those with centric and whole electrodes, respectively, and the amplitude of a partially-etched ZnO film pMUT under a certain voltage is 5.5 dB and 30 dB higher than those with centric and whole electrode, respectively. The pMUT was fabricated by standard bulk micromachining fabrication techniques. The piezoelectric ZnO films were deposited by direct current magnetron sputtering and exhibit a densely packed structure with columnar crystallites preferentially oriented along the (002) plane. Both receive and transmit sensitivity were measured in absolute ethanol. The test results show that the removal of outer-ring ZnO films can raise the sensitivity notably. The receive sensitivity and transmit sensitivity of a pMUT with partially-etched ZnO film are separately −238.35 dB (ref. 1 V/µPa) and 150.42 dB (ref. 1 µPa/V), which are significantly higher than those with whole ZnO films.

References

1. Pedersen, T.; Zawada, T.; Hansen, K.; Lou-Moeller, R.; Thomsen, E. Fabrication of High-Frequency pMUT Arrays on Silicon Substrates. *IEEE Trans. Ultrason. Ferroelectr. Freq. Control* **2010**, *57*, 1470–1477. [CrossRef] [PubMed]

2. Akasheh, F.; Myers, T.; Fraser, J.D.; Bose, S.; Bandyopadhyay, A. Development of piezoelectric micromachined ultrasonic transducers. *Sens. Actuators A Phys.* **2004**, *111*, 275–287. [CrossRef]

3. Eccardt, P.C.; Niederer, K. Micromachined ultrasound transducers with improved coupling factors from a CMOS compatible process. *Ultrasonics* **2000**, *38*, 774–780. [CrossRef]

4. Savoia, A.S.; Caliano, G.; Lula, A.; Pappalardo, M. Design and Fabrication of a cMUT Probe for Ultrasound Imaging of Fingerprints. In Proceedings of the IEEE International Ultrasonics Symposium, San Diego, CA, USA, 11–14 October 2010; pp. 1877–1880.

5. Tang, H.; Lu, Y.; Fung, S.; Tsai, J.M.; Daneman, M.; Horsley, D.A.; Boser, B.E. Pulse-echo ultra-sonic fingerprint sensor on a chip. In Proceedings of the International Conference on Solid-State Sensors, Actuators and Microsystems, Anchorage, AK, USA, 21–25 June 2015; pp. 674–677.

6. Jiang, X.; Tang, H.; Lu, Y.; Ng, E.J.; Tsai, J.M.; Daneman, M.J.; Boser, B.E.; Horsley, D.A. Inter-element coupling effects in pulse-echo ultrasonicfingerprint sensors. In Proceedings of the IEEE 30th International Conference on Micro Electro Mechanical Systems (MEMS), Las Vegas, NV, USA, 22–26 January 2017; pp. 1192–1195.

7. Kuo, J.C.; Hoople, J.T.; Abdelmejeed, M.; Abdel-moneum, M.; Lal, A. 64-Pixel solid state CMOS com-patible ultrasonic fingerprint reader. In Proceedings of the IEEE 30th International Conference on Micro Electro Mechanical Systems (MEMS), Las Vegas, NV, USA, 22–26 January 2017; pp. 9–12.

8. Horsley, D.A.; Lu, Y.; Tang, H.; Jiang, X.; Bose, B.E.; Tsai, J.M.; Ng, E.J.; Daneman, M.J. Ultrasonic fingerprint sensor based on a PMUT array bonded to CMOS circuitry. In Proceedings of the IEEE International Ultrasonics Symposium (IUS), Tours, France, 18–21 September 2016; pp. 1–4.

9. Jiang, X.; Tang, H.; Lu, Y.; Li, X.; Tsai, J.M.; Ng, E.J.; Daneman, M.J.; Lim, M.; Assaderaghi, F.; Boser, B.E.; et al. Monolithic 591 × 438 DPI ultrasonic fingerprint sensor. In Proceedings of the IEEE 29th International Conference on Micro Electro Mechanical Systems (MEMS), Shanghai, China, 24–28 January 2016.

10. Horsley, D.A.; Rozen, O.; Lu, Y.; Shelton, S.; Guedes, A.; Przybyla, R.; Tang, H.; Boser, B.E. Piezoelectric Micromachined Ultrasonic Transducers for Human-Machine Interfaces and Biometric Sensing. In Proceedings of the IEEE SENSORS, Busan, Korea, 1–4 November 2015; pp. 1–4.

11. Mohamed, H.; Polla, D.; Ebbini, E.; Zurn, S. Micromachined Piezoelectric Ultrasonic Imaging Transducer. In Proceedings of the Microelectromechanical Systems Conference, Berkeley, CA, USA, 24–26 August 2001; pp. 95–98.

12. Baborowski, J.; Muralt, P.; Ledermann, N.; Petitgrand, S.; Bosseboeuf, A.; Setter, N.; Gaucher, P. PZT coated membrane structures for micromachined ultrasonic transducers. In Proceedings of the 13th IEEE International Symposium on Applications of Ferroelectrics, Nara, Japan, 1 June 2002; pp. 483–486.

13. Zhu, B.P.; Wu, D.W.; Zhang, Y.; Ou-Yang, J.; Chen, S.; Yang, X.F. Sol-gel derived PMN–PT thick films for high frequency ultrasound linear array applications. *Ceram. Int.* **2013**, *39*, 8709–8714. [CrossRef]

14. Wang, C.; Wang, Z.; Ren, T.; Zhu, Y.; Yang, Y.; Wu, X.; Wang, H.; Fang, H.; Liu, L. A Micromachined Piezoelectric Ultrasonic Transducer Operating in d_{33} Mode Using Square Interdigital Electrodes. *IEEE Sens. J.* **2007**, *7*, 967–976. [CrossRef]

15. Yaacob, M.I.H.; Arshad, M.R.; Manaf, A.A. Modeling and theoretical characterization of circular pMUT for immersion applications. In Proceedings of the IEEE OCEANS, Sydney, Australia, 24–27 May 2010; pp. 1–4.

16. Perçin, G.; Khuri-Yakub, B.T. Piezoelectrically actuated flextensional micromachined ultrasound transducers. *Ultrasonics* **2002**, *40*, 441–448. [CrossRef]

17. Wang, Z.; Miao, J.; Zhu, W. Micromachined ultrasonic transducers and arrays based on piezoelectric thick film. *Appl. Phys. A* **2008**, *91*, 107–117. [CrossRef]

18. Bathurst, S.P.; Kim, S.G. Printing of uniform PZT thin films for MEMS applications. *CIRP Ann. Manuf. Technol.* **2013**, *62*, 227–230. [CrossRef]

19. Lu, Y.; Horsley, D.A. Modeling, Fabrication, and Characterization of Piezoelectric Micromachined Ultrasonic Transducer Arrays Based on Cavity SOI Wafers. *J. Microelectromech. Syst.* **2015**, *24*, 1142–1149. [CrossRef]

20. Hedegaard, T.; Pedersen, T.; Thomsen, E.V.; Lou-Moeller, R.; Hansen, K.; Zawada, T. Screen printed thick film based pMUT arrays. In Proceedings of the IEEE Ultrasonics Symposium, Beijing, China, 2–5 November 2008; pp. 2126–2129.

21. Jayaraman, V.K.; Kuwabara, Y.M.; Álvarez, A.M.; Amador, M.d.l.l.O. Importance of substrate rotation speed on the growth of homogeneous ZnO thin films by reactive sputtering. *Mater. Lett.* **2016**, *169*, 1–4.

22. Suzuki, T.; Chiba, H.; Kawashima, T.; Washio, K. Comparison study of V-doped ZnO thin films on polycarbonate and quartz substrates deposited by RF magnetron sputtering. *Thin Solid Films* **2016**, *605*, 53–56. [CrossRef]

23. Bhatia, D.; Roy, S.; Nawaz, S.; Palkar, V.R. Observation of temperature effect on electrical properties of novel $Au/Bi_{0.7}Dy_{0.3}FeO_3/ZnO/p$-Si thin film MIS capacitor for MEMS applications. *Microelectron. Eng.* **2017**, *168*, 55–61. [CrossRef]

24. Arya, S.; Khan, S.; Kumar, S.; Lehana, P. Design and fabrication of MEMS based electrostatic cantilever as ultrasonic signal generator. *Microelectron. Eng.* **2016**, *154*, 74–79. [CrossRef]

25. Tue, P.T.; Shimoda, T.; Takamura, Y. Fine-patterning of sol-gel derived PZT film by a novel lift-off process using solution-processed metal oxide as a sacrificial layer. *Ceram. Int.* **2016**, *42*, 18431–18435. [CrossRef]

26. Li, J.; Ren, W.; Wang, C.; Liu, M.; Fan, G. Micro-patterning of PZT thick film by lift-off using ZnO as a sacrificial layer. *Ceram. Int.* **2015**, *41*, 7325–7328. [CrossRef]

27. Wang, Z.; Miao, J.; Zhu, W. Piezoelectric thick films and their application in MEMS. *J. Eur. Ceram. Soc.* **2007**, *27*, 3759–3764. [CrossRef]

28. Belgacem, B.; Calame, F.; Muralt, P. Thick PZT sol-gel films for pMUT transducers performances improvement. In Proceedings of the IEEE International Ultrasonics Symposium, Vancouver, BC, Canada, 3–6 October 2006; pp. 922–925.

29. Yamashita, K.; Watanabe, T.; Yoshizaki, T.; Noda, M.; Okuyama, M. Buckling control of silicon dioxide diaphragms by lateral stress enhancement for sensitivity improvement of piezoelectric ultrasonic microsensors. *Sens. Actuators A Phys.* **2011**, *165*, 54–58. [CrossRef]

30. Wang, Z.; Zhu, W.; Miao, J.; Zhu, H.; Chao, C.; Tan, O.K. Micromachined thick film piezoelectric ultrasonic transducer array. *Sens. Actuators A Phys.* **2006**, *130–131*, 485–490. [CrossRef]

31. Dausch, D.E.; Gilchrist, K.H.; Castellucci, J.B.; Chou, D.R. Performance of Flexure-Mode pMUT 2D Arrays. In Proceedings of the IEEE Ultrasonics Symposium, New York, NY, USA, 28–31 October 2007.

32. Lu, Y.; Tang, H.; Fung, S.; Boser, B.E.; Horsley, D.A. Pulse-Echo Ultrasound Imaging Using an AlN Piezoelectric Micromachined Ultrasonic Transducer Array With Transmit Beam-Forming. *J. Microelectromech. Syst.* **2016**, *25*, 179–187. [CrossRef]

33. Yaacob, M.I.H.; Arshad, M.R.; Manaf, A.A. Theoretical characterization of square piezoelectric micro ultrasonic transducer for underwater applications. In Proceedings of the 7th International Symposium on Mechatronics and its Applications, Sharjah, UAE, 20–22 April 2010; pp. 1–5.

34. Dausch, D.E.; Cstellucci, J.B.; Chou, D.R.; von Ramm, O.T. Piezoelectric Micromachined Ultrasound Transducer (pMUT) Arrays for 3D Imaging Probes. In Proceedings of the IEEE Ultrasonics Symposium, Vancouver, BC, Canada, 3–6 October 2006; pp. 934–937.

35. Iguchi, S. Die Biegungsschwingungen der vierseitig eingespannten rechteckigen Platte. *Ing. Arch.* **1937**, *8*, 11–25. [CrossRef]

36. Li, J.; Wang, C.; Ren, W.; Ma, J. ZnO thin film piezoelectric micromachined microphone with symmetric composite vibrating diaphragm. *Smart Mater. Struct.* **2017**, *26*, 1–10. [CrossRef]

37. Stanimirović, Z.; Stanimirović, I. Mechanical characterization of MEMS materials. In Proceedings of the 28th International Conference on Microelectronics, Nis, Serbia, 13–16 May 2012; pp. 177–179.

38. Jiang, W.; Xu, D.; Yao, S.; Xiong, B.; Wang, Y. Effect of hyperthermal annealing on LPCVD silicon nitride. *Mater. Sci. Semicond. Process.* **2016**, *43*, 222–229. [CrossRef]

39. Lee, W.S.; Lee, S.S. Piezoelectric microphone built on circular diaphragm. *Sens. Actuators A Phys.* **2008**, *144*, 367–373. [CrossRef]

40. Dehé, A.; Wurzer, M.; Füldner, M.; Krumbein, U. Design of a Poly Silicon MEMS Microphone for High Signal-to-Noise Ratio. In Proceedings of the European Solid-State Device Research Conference, Bucharest, Romania, 16–20 September 2013; pp. 292–295.

41. Li, J.; Wang, C.; Ma, J.; Liu, M. Micromachined ultrasonic transducers based on lead zirconate titanate (PZT) films. *Microsyst. Technol.* **2013**, *19*, 211–218. [CrossRef]